SocialNav-Map: Dynamic Mapping with Human Trajectory Prediction for Zero-Shot Social Navigation

Lingfeng Zhang^{1,2,3}, Erjia Xiao⁴, Xiaoshuai Hao^{3,†}, Haoxiang Fu⁵, Zeying Gong⁴ Long Chen³, Xiaojun Liang^{2,≅}, Renjing Xu⁴, Hangjun Ye³, Wenbo Ding^{1,≅}

¹Shenzhen Tsinghua International Graduate School, Tsinghua Univeristy
 ²Peng Cheng Laboratory, ³Xiaomi EV
 ⁴The Hong Kong University of Science and Technology (Guangzhou)
 ⁵National University of Singapore

zlf25@mails.tsinghua.edu.cn, ding.wenbo@sz.tsinghua.edu.cn

Abstract—Social navigation in densely populated dynamic environments poses a significant challenge for autonomous mobile robots, requiring advanced strategies for safe interaction. Existing reinforcement learning (RL)-based methods require over 2000+ hours of extensive training and often struggle to generalize to unfamiliar environments without additional finetuning, limiting their practical application in real-world scenarios. To address these limitations, we propose SocialNav-Map, a novel zero-shot social navigation framework that combines dynamic human trajectory prediction with occupancy mapping, enabling safe and efficient navigation without the need for environment-specific training. Specifically, SocialNav-Map first transforms the task goal position into the constructed map coordinate system. Subsequently, it creates a dynamic occupancy map that incorporates predicted human movements as dynamic obstacles. The framework employs two complementary methods for human trajectory prediction: history prediction and orientation prediction. By integrating these predicted trajectories into the occupancy map, the robot can proactively avoid potential collisions with humans while efficiently navigating to its destination. Extensive experiments on the Social-HM3D and Social-MP3D datasets demonstrate that SocialNav-Map significantly outperforms state-of-the-art (SOTA) RL-based methods, which require 2,396 GPU hours of training. Notably, it reduces human collision rates by over 10% without necessitating any training in novel environments. By eliminating the need for environment-specific training, SocialNav-Map achieves superior navigation performance, paving the way for the deployment of social navigation systems in real-world environments characterized by diverse human behaviors. The code is available at: https://github.com/linglingxiansen/SocialNav-Map.

I. INTRODUCTION

Autonomous robots in densely populated environments face significant social navigation challenges, needing to achieve navigation goals while respecting social norms and ensuring human comfort [1], [2], [3], [4]. This issue is especially critical indoors, where limited space, unpredictable human behavior, and complex layouts create dynamic obstacles that traditional navigation systems struggle to manage effectively [5], [6], [7], [8], [9], [10], [11], [12].

The current approach to Social Navigation (SocialNav) primarily utilizes reinforcement learning (RL) [13], [14],

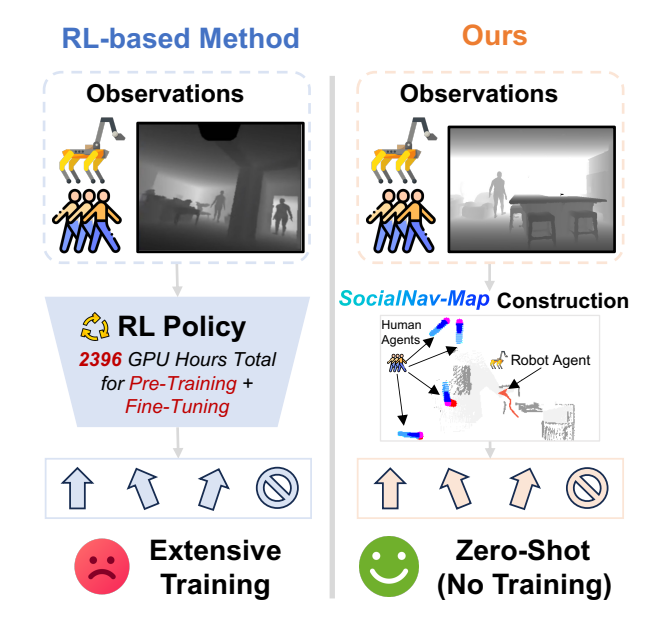


Fig. 1: Comparison of reinforcement learning-based social navigation methods and our *SocialNav-Map* framework. Traditional reinforcement learning (RL)-based methods necessitate extensive training—totaling 2,396 GPU hours—through trial-and-error in simulated environments prior to deployment. In contrast, we present *SocialNav-Map*, a zero-shot social navigation framework that tackles social navigation tasks by constructing dynamic occupancy maps and predicting human trajectories. Notably, *SocialNav-Map* achieves superior performance compared to state-of-the-art RL-based methods, all without the need for any training.

[15], [16], [17], wherein agents develop navigation policies through extensive interactions within simulated environments. Despite showing potential in controlled settings, RL methods encounter significant limitations that impede practical deployment. They typically require extensive training periods—often several weeks—to formulate effective policies for specific environments, and these policies often struggle to generalize to new contexts with different layouts, human densities, or behaviors, necessitating costly retraining [18],

[†] Project Leader.

[™] Corresponding Authors.

[16], [19], [20], [21]. This generalization issue is worsened by the reactive nature of most RL systems, which tend to prioritize immediate obstacle avoidance over long-term strategic planning. In complex scenarios, such as busy intersections or heavily trafficked corridors, these short-sighted strategies can result in inefficient navigation, deadlocks, or socially inappropriate behaviors that may discomfort those nearby [22], [23]. Recent advancements in human trajectory prediction offer a promising alternative, allowing robots to move from passive to active navigation strategies by forecasting future human movements, thereby enhancing social acceptance and navigation efficiency. However, trajectory prediction in indoor environments presents challenges, including limited prediction ranges due to frequent directional changes, complex layouts that restrict movement, and high interaction densities that require precise collision avoidance [24], [25], [26], [27], [28].

As shown in Fig. 1, researchers recently proposed Falcon [18], a future-oriented framework that integrates explicit trajectory prediction into reinforcement learning-based SocialNav. Their approach effectively demonstrates the advantages of incorporating human trajectory prediction through auxiliary tasks during training, achieving state-of-the-art performance on the SocialNav benchmark. However, Falcon still requires extensive reinforcement learning training—totaling 2,396 GPU hours for pre-training (2,204 hours) [29] and fine-tuning (192 hours) [18]—and faces generalization challenges when deployed in new environments, necessitating additional fine-tuning for optimal performance.

To address this challenge, we present *SocialNav-Map*, as shown in Fig. 1, a zero-shot SocialNav framework that eliminates the need for environment-specific training while outperforming state-of-the-art reinforcement learning methods [5]. [6], [30], [7], [31]. Our framework begins by transforming the task goal location into a constructed map coordinate system. It then creates a socially aware dynamic occupancy map that integrates predicted human motion trajectories as dynamic obstacles, employing a structured process to enhance navigation efficiency and safety. Specifically, the core innovation of our approach lies in a fused trajectory prediction system that integrates two complementary methods: historical prediction, which analyzes patterns derived from observed human motion, and orientation prediction, which infers future trajectories based on current human pose and orientation. Utilizing these predictions, we treat both past and anticipated human trajectories as dynamic obstacles within the occupancy map, enabling proactive navigation decisions rather than merely reactive obstacle avoidance. Past and predicted human positions are incorporated into the occupancy map as dynamic obstacles that are gradually updated over time. This design ensures that navigation decisions account for potential future human positions while preventing outdated predictions from creating persistent obstacles, which could lead to overly cautious or inefficient robot behavior. Extensive experiments demonstrate that our zero-shot Social-Nav framework can effectively complete tasks in dynamic social scenarios without any prior training, achieving stateof-the-art performance comparable to reinforcement learning methods that require significant training (*totaling 2,396 GPU hours*). This underscores the performance and generalization capabilities of our approach.

The main contributions of our paper are as follows:

- We propose SocialNav-Map, a zero-shot social navigation framework capable of effectively solving social navigation tasks in dynamic environments without the need for environment-specific training.
- We develop two complementary zero-shot human trajectory prediction methods: historical motion pattern analysis and orientation-based linear extrapolation, both of which effectively forecast future human trajectories.
- We introduce a dynamic obstacle management system that treats both the current and predicted human positions as dynamic obstacles and employs an adaptive decay mechanism to achieve efficient obstacle avoidance and navigation.
- Extensive experiments demonstrate that our SocialNav-Map achieves SOTA performance while reducing human collision rates by over 10% without any training, and can be generalized to any scenario.

II. RELATED WORK

A. Social Navigation

Social Navigation (SocialNav) [2], [3], [4], [32] is a challenging robotics task that requires autonomous agents to navigate safely and efficiently in an environment where humans are moving and reach a specified target location. The main goal is to enable robots to understand, predict, and appropriately respond to human behavior, ensuring collisionfree navigation while respecting social norms and personal space. Various methods have been developed to address the challenges of social navigation. Reinforcement learningbased methods [20], [17], [18], [22] train agents through extensive interactions with a simulated environment and learn collision avoidance behaviors through trial and error. Multiagent coordination methods [33], [34] model the navigation problem as a distributed planning task where multiple agents coordinate their motion. Graph-based methods [33], [34], [35], [9] represent human-robot interactions through spatiotemporal graphs to capture agent dynamics and predict future motion over time. Recent studies have also explored egocentric navigation in photorealistic environments [36], [37], [31], [38], focusing on first-person perception and decision-making. Falcon helps agents perform safe social navigation by predicting human trajectories as auxiliary information. However, these methods typically require thousands of hours of training and struggle to generalize to new environments. Unlike existing methods that rely on extensive environment-specific training, our approach introduces a zero-shot framework that combines occupancy mapping, trajectory prediction, and dynamic human obstacle mapping, enabling effective social navigation without requiring pretraining in the target environment.

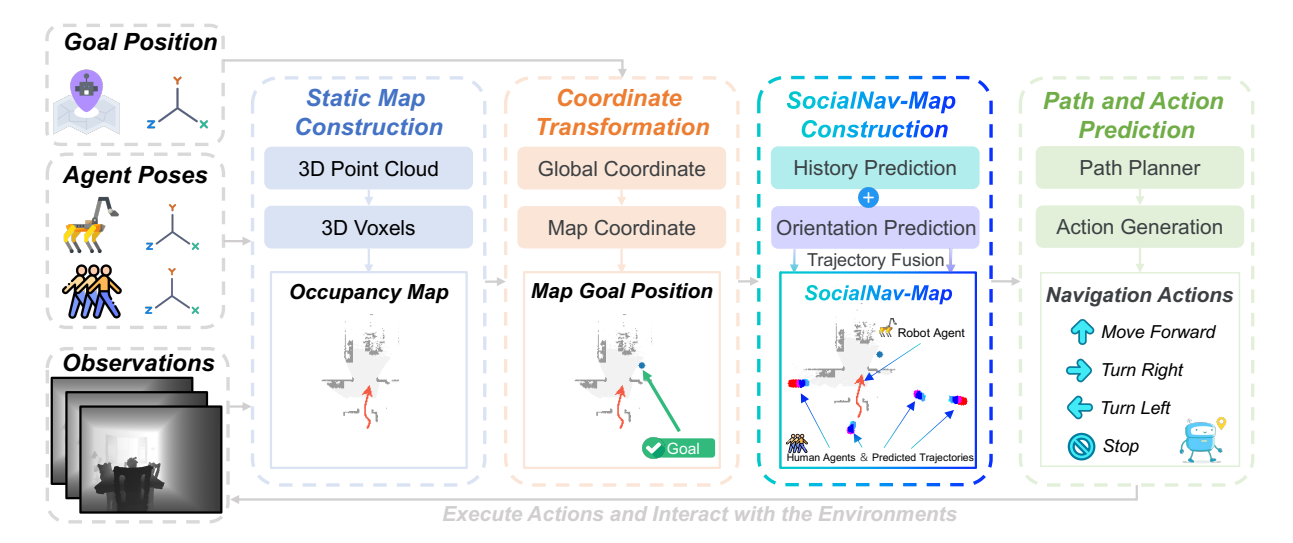


Fig. 2: The general pipeline of our *SocialNav-Map* framework. The system first constructs a static occupancy map from observation data through 3D point cloud generation and voxel discretization, then converts target locations into map coordinates. The core of *SocialNav-Map* employs dual trajectory prediction—history prediction analyzes past human motion patterns, while direction prediction infers future positions—and fuses these predictions with dynamic obstacles with time decay. Finally, a fast marching method generates optimal collision-free paths and converts them into discrete navigation actions for zero-shot social navigation.

B. Zero-Shot Embodied Navigation

Zero-Shot Embodied Navigation (ZSEN) has become a promising paradigm, addressing the limitations of learningbased approaches: these methods require extensive training, suffer from poor generalization, and struggle to adapt to new environments [21], [20], [39], [40]. For Object Navigation (ObjectNav), methods like CoW [41] and ESC [42] use CLIP [43] for exploration and object detection. L3MVN [44], TriHelper [5], MFNP [6], and VLFM [45] use semantic value map-based approaches for exploration and task completion. For Vision-and-Language Navigation (VLN), methods like NavGPT [46], DiscussNav [47], and NavCoT [48] use large models for inference and action generation. Navid [49], MapNav [50], and NaVILA [51] use Vision-Language Models (VLMs) as a backbone for end-to-end training and deployment. InstrucNav [52] and UniGoal [53] can simultaneously address both ObjectNav and VLN tasks. However, all previous methods are unable to directly address SocialNav task and handle dynamic human obstacles. We propose a zero-shot SocialNav framework and dynamic human obstacle occupancy map construction for the first time.

III. METHODOLOGY

A. Problem Formulation

The Social Navigation (SocialNav) task requires agents to navigate safely and efficiently to designated goal locations in environments populated by dynamic humans. The task is defined within scene S containing N moving humans $\mathcal{H} = \{h_1, h_2, ..., h_N\}$, where each human h_i follows a trajectory $\tau_i(t)$ with position and orientation evolving over time. At the beginning of each episode, the agent is randomly initialized at position p_0 within scene S and is assigned a specific goal location $g \in \mathcal{G}$.

At each discrete time step t, the agent receives an observation vector $\mathcal{O}_t = (V_t, P_t, H_t)$, where V_t represents visual input (depth images), P_t represents the agent's current pose, and H_t represents observable human positions and orientations. Based on these inputs, the agent must select an action $a_t \in \mathcal{A}$, where the action space \mathcal{A} contains four actions: move forward, turn left, turn right, and stop. The agent must navigate toward its goal while maintaining safe distances from both static obstacles and dynamic humans.

Task success is defined by two criteria: (1) the agent reaches within distance threshold d_g of the goal location (typically 0.2 meters), and (2) the agent avoids collisions with humans throughout the episode, defined as maintaining minimum distance d_h from any human (typically 0.1 meters). Each navigation episode is limited to T_{max} time steps (typically 500 steps).

B. Overview

Our *SocialNav-Map* framework operates through a four-stage pipeline that transforms observations $\mathcal{O}_t = (V_t, P_t, H_t)$ into socially-aware navigation actions. The Static Map Construction stage builds an occupancy map from RGB-D observations, while Coordinate Transformation converts the goal position g into map coordinates. The core *SocialNav-Map* Construction employs dual trajectory prediction: history prediction analyzes human motion patterns and orientation prediction extrapolates future positions based on current poses. These predicted trajectories are fused as dynamic obstacles with temporal decay into the occupancy map. Finally, Path and Action Prediction generates collision-free paths and converts them into discrete actions $a_t \in \mathcal{A}$ to achieve safe navigation without environment-specific training.

C. Static Map Construction

The static map construction process transforms RGB-D observations V_t into a 2D occupancy map through a series of geometric transformations. Given a depth image $D \in \mathbb{R}^{H \times W}$ where H and W are image dimensions, we first generate a 3D point cloud using the camera intrinsic matrix K:

$$P_{cam} = K^{-1} \begin{bmatrix} u \cdot D(u, v) \\ v \cdot D(u, v) \\ D(u, v) \end{bmatrix}, \tag{1}$$

where (u,v) are pixel coordinates and D(u,v) is the depth value at pixel (u,v). The camera coordinate points P_{cam} are then transformed to the agent's coordinate frame using the camera height h_{agent} and elevation angle θ_{eve} :

$$P_{agent} = R_x(\theta_{eve}) \cdot P_{cam} + \begin{bmatrix} 0 \\ 0 \\ h_{agent} \end{bmatrix}, \qquad (2)$$

where $R_x(\theta_{eve})$ is the rotation matrix around the x-axis. Next, we apply pose transformation to center the agent's view using shift location $s=\left[\frac{r\cdot res}{2},0,\frac{\pi}{2}\right]$ where r is vision range and res is resolution:

$$P_{centered} = R_z(s_2) \cdot P_{agent} + \begin{bmatrix} s_0 \\ s_1 \\ 0 \end{bmatrix}. \tag{3}$$

The centered 3D points are then discretized into voxel coordinates by normalizing to the range [-1, 1]:

$$P_{voxel} = \frac{2 \cdot (P_{centered} - center)}{range} - 1, \tag{4}$$

where center and range define the voxel grid bounds. Finally, the 3D voxel representation is projected to a 2D occupancy map by summing over height layers within the agent's traversable range $[z_{min}, z_{max}]$:

$$M_{occ}(x,y) = \sum_{z=z_{min}}^{z_{max}} V_{voxel}(x,y,z).$$
 (5)

The resulting occupancy map M_{occ} represents obstacles as high-confidence regions where depth measurements indicate solid surfaces within the agent's navigation height range.

D. Coordinate Transformation

The coordinate transformation stage establishes a consistent spatial reference by converting goal positions from world coordinates to map coordinates and maintaining fixed spatial relationships throughout navigation. Given the goal position in world coordinates $g_{world} = [x_w, y_w, z_w]$ and the agent's initial position $p_{init} = [x_{init}, y_{init}, z_{init}]$, the system first transforms world coordinates to simulator coordinates using:

$$g_{sim} = \begin{bmatrix} -z_w \\ -x_w \\ y_w \end{bmatrix}, \quad p_{sim} = \begin{bmatrix} -z_{init} \\ -x_{init} \\ y_{init} \end{bmatrix}. \tag{6}$$

The relative offset between goal and agent in simulator

coordinates is computed as:

$$\Delta_{sim} = g_{sim} - p_{sim} = \begin{bmatrix} -(z_w - z_{init}) \\ -(x_w - x_{init}) \\ y_w - y_{init} \end{bmatrix}.$$
 (7)

This offset is then mapped to the global map coordinate system, where the agent's initial position is fixed at the map center $p_{map_center} = \left[\frac{W_{map}}{2}, \frac{H_{map}}{2}\right]$ with W_{map} and H_{map} representing map dimensions in meters. The goal's global map position is calculated as:

$$g_{global_map} = p_{map_center} + \begin{bmatrix} -\Delta_{sim}[0] \\ \Delta_{sim}[1] \end{bmatrix}.$$
 (8)

For dynamic trajectory prediction, human positions $h_{world} = [x_h, y_h, z_h]$ undergo the same transformation pipeline using the fixed initial agent reference frame:

$$h_{global_map} = p_{map_center} + \begin{bmatrix} -(-z_h + z_{init}) \\ -(-x_h + x_{init}) \end{bmatrix}. \quad (9)$$

When the transformed goal position falls outside the current local map boundaries, the system places an intermediate goal in the direction of the true goal to maintain navigation progress. The system calculates the direction vector from the agent's current position to the out-of-bounds goal and places an intermediate target at distance $d_{\rm intermediate} = \min(W_{\rm local}/3, H_{\rm local}/3)$ along this direction:

$$g_{\text{intermediate}} = a_{\text{local}} + \frac{g_{\text{local}} - a_{\text{local}}}{||g_{\text{local}} - a_{\text{local}}||} \times d_{\text{intermediate}}, \quad (10)$$

where coordinates are clamped to remain within safe map boundaries $[3, map_{size} - 4]$.

This coordinate transformation ensures spatial consistency by maintaining a fixed reference frame anchored to the agent's initial position, enabling accurate goal localization and human trajectory prediction regardless of the agent's current location during navigation.

E. SocialNav-Map Construction

The general pipeline of our *SocialNav-Map* Construction is illustrated in Fig. 2 and Fig. 3. The *SocialNav-Map* construction integrates dual trajectory prediction methods to anticipate human movements. The system maintains historical position data $H_i = \{(p_t, t)\}$ for each human agent i, where $p_t = [x_t, y_t]$ represents position at timestep t.

History Prediction For agents with sufficient trajectory history (length ≥ 2), the system performs linear regression on historical positions. Given position sequence $\{p_{t-n},...,p_{t-1},p_t\}$ with corresponding timesteps $\{t-n,...,t-1,t\}$, the future trajectory is predicted using:

$$\hat{p}_{t+k}^{hist} = \begin{bmatrix} a_x \cdot (t+k) + b_x \\ a_y \cdot (t+k) + b_y \end{bmatrix},\tag{11}$$

where (a_x, b_x) and (a_y, b_y) are linear coefficients obtained via least squares fitting over the historical trajectory data.

Orientation Prediction For each human with current orientation θ_i , the system predicts future positions along the

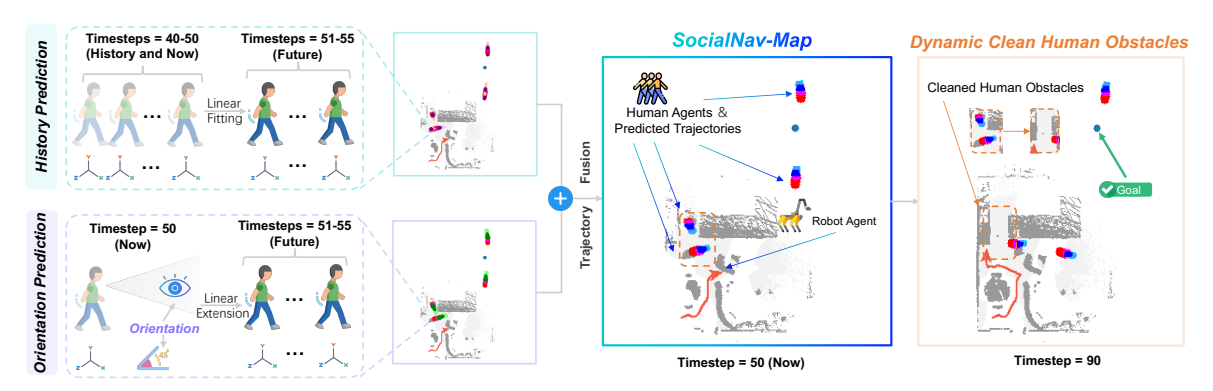


Fig. 3: **Human trajectory prediction and dynamic obstacle management in** *SocialNav-Map*. History prediction analyzes past human motion and uses linear regression fitting to infer future trajectories. Orientation prediction uses the current human pose and orientation to predict future positions via linear extension. These two prediction methods are fused to generate comprehensive trajectory predictions, which are integrated into the occupancy map as dynamic obstacles. These predicted human obstacles are automatically removed from the map after a certain decay period, preventing outdated predictions from hindering robot navigation while ensuring safety during active human movement.

heading direction:

$$\hat{p}_{t+k}^{orient} = p_t + k \cdot d_{step} \cdot \begin{bmatrix} \cos(\theta_i + \pi/2) \\ -\sin(\theta_i + \pi/2) \end{bmatrix}, \quad (12)$$

where d_{step} is the step distance and the angle adjustment accounts for coordinate system transformation.

Trajectory Fusion The two prediction methods are fused using adaptive weighting that favors orientation prediction for longer horizons. The fused trajectory is computed as:

$$\hat{p}_{t+k}^{fused} = w_k^{hist} \cdot \hat{p}_{t+k}^{hist} + w_k^{orient} \cdot \hat{p}_{t+k}^{orient}, \qquad (13)$$

where $w_k^{hist} = w_{base} \cdot \alpha^k$ represents diminishing historical influence with decay factor α , and $w_k^{orient} = 1 - w_k^{hist}$ ensures complementary weighting. This fusion approach leverages historical patterns for near-term predictions while relying on orientation-based extrapolation for longer-term forecasting, providing robust trajectory estimation across varying prediction horizons.

Dynamic Human Obstacles The system integrates both predicted trajectories and historical human presence into the occupancy map through morphological operations and temporal decay mechanisms. Human obstacle integration operates on two levels: immediate presence tracking and predictive obstacle placement. Current human positions and predicted trajectory points are converted to occupancy map obstacles using morphological dilation with radius $r_{human} = 0.25$ meters. For each human position p_{human} in global map coordinates, the system creates circular obstacle regions:

$$\mathcal{O}_{human}(x,y) = \{(x,y) : ||[x,y] - p_{human}||_2 \le r_{human}\}.$$
(14)

The occupancy map is updated by setting $M_{occ}(x,y) = 1$ for all positions within the dilated regions using a disk-shaped structuring element S_{disk} with radius $r_{pixels} = r_{human} \cdot 100/res_{map}$.

To prevent stale obstacles from impeding navigation, the system employs a temporal decay mechanism. Each obstacle position is tagged with timestamp t_{create} and removed after

decay period $T_{decay} = 5$ timesteps:

$$M_{occ}(x,y) = \begin{cases} 1 & \text{if } t_{current} - t_{create} \le T_{decay} \\ 0 & \text{if } t_{current} - t_{create} > T_{decay} \end{cases}.$$
 (15)

Expired obstacles are actively cleared through inverse morphological operations, ensuring previously occupied areas become traversable again. The system maintains separate tracking for active obstacles (recently observed) and expired obstacles (beyond decay time), applying dilation for active regions and explicit clearance for expired regions. This approach balances safety by maintaining obstacles around recent human activity while ensuring long-term navigability by removing outdated restrictions.

F. Path and Action Prediction

The path and action prediction stage converts the socially-aware occupancy map into executable navigation commands through hierarchical planning. The system employs Fast Marching Method (FMM) [54] for optimal path generation followed by deterministic action selection.

Path Planner The plath planner operates on the enhanced occupancy map M_{occ} that incorporates static obstacles, dynamic human obstacles, and collision history. The planner first creates a traversability map T(x,y) by applying morphological erosion to account for robot dimensions:

$$T(x,y) = \neg(\text{binary_dilation}(M_{occ}, S_{robot})),$$
 (16)

where S_{robot} is a disk-shaped structuring element representing the robot's footprint. The goal region $\mathcal G$ is dilated using structuring element S_{goal} to create a multi-goal target, and the path planner algorithm computes the distance field D(x,y) by solving the Eikonal equation $|\nabla D|=1/T$ with boundary condition D(g)=0 for all $g\in \mathcal G$. The optimal path follows the negative gradient of the distance field, providing the shortest collision-free trajectory to the goal.

Action Generation From the path solution, the system extracts a short-term goal (STG) point p_{stg} along the optimal path at a fixed lookahead distance. The discrete action

Dataset		Method	SR ↑	SPL ↑	PSC ↑	H-Coll ↓	Final Score ↑
Social-HM3D	Rule-Based	A* [55] ORCA [56]	$46.14{\scriptstyle \pm 0.7}\atop38.91{\scriptstyle \pm 0.1}$	$46.14{\scriptstyle \pm 0.7}\atop38.91{\scriptstyle \pm 0.1}$	$90.56{\scriptstyle \pm 0.2}\atop90.55{\scriptstyle \pm 0.4}$	$53.50{\scriptstyle \pm 0.9}\atop 47.52{\scriptstyle \pm 1.7}$	55.09 ± 0.7 51.95 ± 0.9
	RL-Based	Proximity-Aware [22] Falcon [18]	20.11±1.3 53.84±0.6	$18.57{\scriptstyle\pm1.9}\atop49.30{\scriptstyle\pm0.7}$	92.91±0.5 89.47±1.4	$33.99{\pm0.7} \ 41.58{\pm1.1}$	$43.54{\scriptstyle\pm1.0}\atop60.39{\scriptstyle\pm0.8}$
	Zero-Shot	SocialNav-Map (Ours)	51.71 ±0.3	43.91 ±0.5	89.12 ±0.7	30.36 ±0.9	61.21 ±0.5
Social-MP3D	Rule-Based	A* [55] ORCA [56]	$43.85{\scriptstyle \pm 0.3}\atop40.38{\scriptstyle \pm 0.3}$	$43.85{\scriptstyle \pm 0.3}\atop40.38{\scriptstyle \pm 0.3}$	86.74±3.4 91.76±0.4	$57.94{\scriptstyle\pm1.5}\atop47.16{\scriptstyle\pm0.2}$	52.07±0.8 53.15±0.6
	RL-Based	Proximity-Aware [22] Falcon [18]	18.45±1.4 48.47±0.8	$17.09{\scriptstyle\pm2.8}\atop42.08{\scriptstyle\pm0.4}$	$93.37{\scriptstyle \pm 0.9}\atop90.48{\scriptstyle \pm 0.2}$	$32.18{\pm}3.3\\48.53{\pm}1.2$	43.04±0.8 56.19±0.9
	Zero-Shot	SocialNav-Map (Ours)	43.53 ±0.9	37.09 ±0.5	89.30 ±0.2	30.54 ±1.0	56.58 ±0.6

TABLE I: Performance Evaluation of SocialNav Tasks comparing our zero-shot SocialNav-Map framework with Rule-Based and RL-Based Methods on Social-HM3D (upper group) and Social-MP3D (lower group). Data in the table represents percentages. Falcon [18] results are reproduced from our implementation.

 $a_t \in \{move_forward, turn_left, turn_right, stop\}$ is determined by comparing the relative angle θ_{rel} between the robot's current heading θ_{robot} and the direction to STG:

$$\theta_{rel} = (\theta_{robot} - \arctan 2(p_{stg}[0] - p_{robot}[0], p_{stg}[1] - p_{robot}[1]) \mod 360.$$
 (17)

The action selection follows: $turn_right$ if $\theta_{rel} > 15, turn_left$ if $\theta_{rel} < -15, move_forward$ if $|\theta_{rel}| \leq 15$, and stop if the goal is reached or no valid path exists. This deterministic policy ensures consistent navigation behavior while maintaining computational efficiency for real-time execution.

IV. EXPERIMENT

A. Datasets

We evaluate the **SocialNav-Map** framework on the Social-HM3D and Social-MP3D datasets [18]. These datasets are based on photorealistic HM3D [29] and MP3D [57] scenes and contain simulated environments with real human agents. These datasets contain diverse indoor environments with carefully calibrated human density and incorporate natural motion patterns, where humans alternate between moving and standing still at random walking speeds (0.8-1.2 times the robot speed) and goal-directed trajectories. To demonstrate the zero-shot generalization capability of our method, we perform all evaluations directly on the validation sets of these two datasets without any pre-training or fine-tuning on these environments. Social-HM3D contains 844 scenes and 1087 episodes, while Social-MP3D contains 72 scenes and 317 episodes, comprehensively covering a variety of indoor layouts and human-robot interaction scenarios, enabling a robust evaluation of social navigation performance.

B. Experiment Details

All experiments are conducted using Habitat 3.0 simulator [58] on NVIDIA RTX 3090 GPUs. The occupancy map is constructed with a resolution of 5 cm/pixel and covers a 20m × 20m area. For human trajectory prediction, we use a history length of 10 timesteps and predict 10 future steps with updates every 10 timesteps. The human obstacle radius is set

to 0.25 meters with a temporal decay period of 5 timesteps to balance safety and navigation efficiency. For orientation-based prediction, we project trajectories 0.5 meters ahead with a prediction width of 0.25 meters. The Fast Marching Method (FMM) [54] planner uses morphological dilation with a disk-shaped structuring element (radius 3 pixels) to account for robot dimensions. Episodes are terminated after a maximum of 500 timesteps, with success defined as reaching within 0.2 meters of the goal while maintaining at least 0.1 meters distance from humans.

C. Metrics

Our evaluation metrics build upon existing works [18] and focus on two principal perspectives: task completion and adherence to social navigation objectives. For task completion, we use Success Rate (SR) and Success weighted by Path Length (SPL). For social norms, we evaluate Human-Robot Collision Rate (H-coll) and Personal Space Compliance (PSC). Considering the human collision radius is 0.3m and the robot is 0.25m, the PSC distance threshold is set to 1.0m. To provide a comprehensive assessment of social navigation performance, we introduce a Final Score metric that combines all evaluation dimensions with weights reflecting their relative importance: Final Score = $0.4 \times$ $SR + 0.2 \times SPL + 0.2 \times PSC + 0.2 \times (1 - H\text{-coll})$, where SR and SPL measure navigation effectiveness, PSC evaluates social compliance, and the inverted H-coll term penalizes human collisions. This weighted combination emphasizes task success while ensuring socially appropriate behavior.

D. Baselines

We compare our *SocialNav-Map* framework against established social navigation methods across different algorithmic paradigms. Rule-based methods include A* [55], a classical optimal path planner for static environments, and ORCA [56], which incorporates dynamic collision avoidance with oracle access to agent positions and velocities. RL-based methods comprise Proximity-Aware [22], which introduces auxiliary tasks modeling human distance and direction to capture proximity dynamics, and Falcon [18], the



Fig. 4: Qualitative results of our SocialNav-Map.

Methods	SR↑	SPL↑	PSC↑	H-Coll↓	Final Score↑
SocialNav-Map (Full)	51.71	43.91	89.12	30.36	61.21
w/o Intermediate Goal	49.24	41.18	88.95	32.47	59.15
w/o History Prediction	50.13	42.26	88.74	31.89	59.82
w/o Orientation Prediction	45.87	41.95	88.46	38.12	55.94
w/o Trajectory Fusion	48.69	40.81	88.32	34.58	57.73
w/o Dynamic Obstacles	47.35	39.67	87.29	36.94	56.16

TABLE II: Results of ablation study on Social-HM3D.

recent state-of-the-art future-oriented framework that integrates explicit human trajectory prediction into reinforcement learning, achieving strong performance through auxiliary prediction tasks during training. All methods use only depth observations as visual input to ensure fair comparison. While RL-based baselines require extensive training (2,396 GPU hours for Falcon), our approach operates in a zero-shot manner without any environment-specific training.

E. Compare with SOTA Methods

Tab. I presents the comprehensive evaluation results on both Social-HM3D and Social-MP3D datasets. Our framework achieves remarkable performance compared to stateof-the-art methods while requiring zero training. On Social-HM3D, our method achieves a Final Score of 61.21, slightly outperforming Falcon (60.39) which requires 2396 GPU hours of training. Notably, our approach significantly reduces human collision rates by over 10% compared to Falcon (30.36% vs 41.58%), demonstrating superior social compliance. On Social-MP3D, SocialNav-Map achieves a Final Score of 56.58 compared to Falcon's 56.19, while maintaining the lowest collision rate (30.54% vs 48.53%). These results demonstrate that our framework can match or exceed the performance of heavily trained RL-based methods without requiring any environment-specific training, offering significant practical advantages for real-world deployment.

F. Ablation study

Effect of *SocialNav-Map* We conducted ablation experiments on each component of the *SocialNav-Map* across all episodes in the Social-HM3D dataset, demonstrating the efficacy of each component, the results are shown in Tab II. Removing the intermediate target mechanism causes the final score to drop from 61.21 to 59.15, while removing history prediction and direction prediction results in scores of 59.82 and 58.94, respectively, demonstrating the critical importance of both trajectory prediction methods. The trajectory fusion

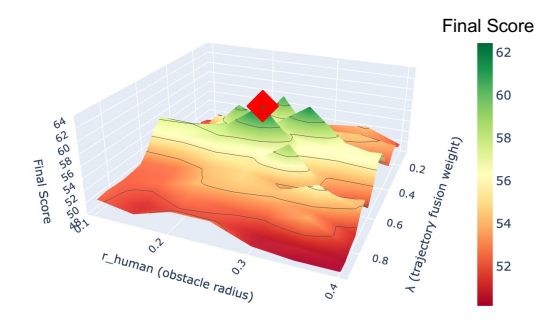


Fig. 5: Hyperparameter Ablation Study on Social-HM3D.

component is crucial, with its removal reducing the score to 57.73, highlighting the advantage of combining prediction methods with adaptive weighting. Most importantly, removing dynamic obstacles results in the largest performance drop, to 56.16, confirming that integrating predicted human trajectories as dynamic obstacles is crucial for safe social navigation. These results verify that each component meaningfully contributes to the overall system performance and works together to achieve superior zero-shot social navigation capabilities.

Effect of Hyperparameters We analyzed key hyperparameters in our SocialNav-Map framework, focusing on the human obstacle radius (r_{human}) and trajectory fusion weight (α) . As shown in Fig. 5, optimal performance occurs at $r_{human}=0.25$ meters and $\alpha=0.5$, achieving a peak Final Score of approximately 61.2. The human obstacle radius defines a safety buffer around predicted human positions; smaller values may lead to unsafe navigation, while larger values result in excessive caution. The trajectory fusion weight α effectively balances history-based and orientation-based predictions, with $\alpha=0.5$ providing the best integration of both approaches.

G. Qualitative Analysis

Fig. 4 demonstrates the effectiveness of our *SocialNav-Map* framework across two navigation episodes. The figure shows the robot successfully avoiding multiple human obstacles while advancing toward its goal. The dynamic occupancy map demonstrates how predicted human trajectories can be integrated with dynamic obstacles to enable proactive path planning. In both episodes, the agent efficiently reached its destination while maintaining a safe distance from humans. The social map continuously updates obstacles and

removes outdated predictions to prevent overly conservative behavior. Results demonstrates the effectiveness of our zeroshot social navigation framework.

V. CONCLUSIONS

In this paper, we present SocialNav-Map, an innovative zero-shot social navigation framework that requires no training for specific environments while achieving stateof-the-art performance. Our approach combines dynamic occupancy mapping with a dual human trajectory prediction system—history and orientation prediction—to effectively avoid collisions in densely populated settings. Unlike existing reinforcement learning methods that demand 2,396 GPU hours of training, our framework outperforms previous state-of-the-art methods on Social-HM3D and Social-MP3D while reducing human collision rates by over 10%. By treating predicted human trajectories as dynamic obstacles and employing a temporal decay mechanism, SocialNav-Map excels across multiple datasets without fine-tuning, successfully addressing the generalization limitations of existing approaches and paving the way for practical deployment of social navigation systems in real-world environments with diverse human behaviors.

REFERENCES

- C. Mavrogiannis, F. Baldini, A. Wang, D. Zhao, P. Trautman, A. Steinfeld, and J. Oh, "Core challenges of social robot navigation: A survey," ACM Transactions on Human-Robot Interaction, pp. 1–39, 2023.
- [2] C. Pérez-D'Arpino, C. Liu, P. Goebel, R. Martín-Martín, and S. Savarese, "Robot navigation in constrained pedestrian environments using reinforcement learning," in *IEEE International Conference on Robotics and Automation*, 2021, pp. 1140–1146.
- [3] A. Francis, C. Pérez-d'Arpino, C. Li, F. Xia, A. Alahi, R. Alami, A. Bera, A. Biswas, J. Biswas, R. Chandra *et al.*, "Principles and guidelines for evaluating social robot navigation algorithms," *arXiv* preprint arXiv:2306.16740, 2023.
- [4] E. Xiao, L. Zhang, Y. Tang, H. Cheng, R. Xu, W. Ding, L. Zhou, L. Chen, H. Ye, and X. Hao, "Team xiaomi ev-ad vla: Learning to navigate socially through proactive risk perception-technical report for iros 2025 robosense challenge social navigation track," arXiv preprint arXiv:2510.07871, 2025.
- [5] L. Zhang, Q. Zhang, H. Wang, E. Xiao, Z. Jiang, H. Chen, and R. Xu, "Trihelper: Zero-shot object navigation with dynamic assistance," in *IEEE/RSJ International Conference on Intelligent Robots and Systems*, 2024, pp. 10 035–10 042.
- [6] L. Zhang, H. Wang, E. Xiao, X. Zhang, Q. Zhang, Z. Jiang, and R. Xu, "Multi-floor zero-shot object navigation policy," in *IEEE International Conference on Robotics and Automation*, 2025, pp. 6416–6422.
- [7] L. Zhang, X. Hao, Q. Xu, Q. Zhang, X. Zhang, P. Wang, J. Zhang, Z. Wang, S. Zhang, and R. M. Xu, "A novel memory representation via annotated semantic maps for vlm-based vision-and-language navigation," arXiv preprint arXiv:2502.13451, 2025.
- [8] Q. Zhang, Z. Zhang, W. Cui, J. Sun, J. Cao, Y. Guo, G. Han, W. Zhao, J. Wang, C. Sun et al., "Humanoidpano: Hybrid spherical panoramiclidar cross-modal perception for humanoid robots," arXiv preprint arXiv:2503.09010, 2025.
- [9] P. Liu, Q. Zhang, D. Peng, L. Zhang, Y. Qin, H. Zhou, J. Ma, R. Xu, and Y. Ji, "Toponav: Topological graphs as a key enabler for advanced object navigation," arXiv preprint arXiv:2509.01364, 2025.
- [10] X. Hao, W. Zhang, D. Wu, F. Zhu, and B. Li, "Listen and look: Multi-modal aggregation and co-attention network for video-audio retrieval," in 2022 IEEE International Conference on Multimedia and Expo (ICME). IEEE, 2022, pp. 1–6.
- [11] X. Hao, Y. Zhou, D. Wu, W. Zhang, B. Li, W. Wang, and D. Meng, "What matters: Attentive and relational feature aggregation network for video-text retrieval," in 2021 IEEE International Conference on Multimedia and Expo (ICME). IEEE, 2021, pp. 1–6.

- [12] C. Zhang, P. Hao, X. Cao, X. Hao, S. Cui, and S. Wang, "Vtla: Vision-tactile-language-action model with preference learning for insertion manipulation," arXiv preprint arXiv:2505.09577, 2025.
- [13] A. Kapoor, S. Swamy, P. Bachiller, and L. J. Manso, "Socnavgym: a reinforcement learning gym for social navigation," in *IEEE Interna*tional Conference on Robot and Human Interactive Communication, 2023, pp. 2010–2017.
- [14] W. Wang, L. Mao, R. Wang, and B.-C. Min, "Multi-robot cooperative socially-aware navigation using multi-agent reinforcement learning," in *IEEE International Conference on Robotics and Automation*, 2024, pp. 12353–12360.
- [15] N. Hirose, D. Shah, K. Stachowicz, A. Sridhar, and S. Levine, "Selfi: Autonomous self-improvement with reinforcement learning for social navigation," arXiv preprint arXiv:2403.00991, 2024.
- [16] J. Schulman, F. Wolski, P. Dhariwal, A. Radford, and O. Klimov, "Proximal policy optimization algorithms," arXiv preprint arXiv:1707.06347, 2017.
- [17] Q. Zhang, G. Han, J. Sun, W. Zhao, J. Cao, J. Wang, H. Cheng, L. Zhang, Y. Guo, and R. Xu, "Lips: Large-scale humanoid robot reinforcement learning with parallel-series structures," arXiv preprint arXiv:2503.08349, 2025.
- [18] Z. Gong, T. Hu, R. Qiu, and J. Liang, "From cognition to precognition: A future-aware framework for social navigation," in *IEEE International Conference on Robotics and Automation*, 2025, pp. 9122–9129.
- [19] E. Wijmans, A. Kadian, A. Morcos, S. Lee, I. Essa, D. Parikh, M. Savva, and D. Batra, "Dd-ppo: Learning near-perfect pointgoal navigators from 2.5 billion frames," arXiv preprint arXiv:1911.00357, 2019.
- [20] B. R. Team, M. Cao, H. Tan, Y. Ji, X. Chen, M. Lin, Z. Li, Z. Cao, P. Wang, E. Zhou et al., "Robobrain 2.0 technical report," arXiv preprint arXiv:2507.02029, 2025.
- [21] Y. Wu, H. Lyu, Y. Tang, L. Zhang, Z. Zhang, W. Zhou, and S. Hao, "Evaluating gpt-4o's embodied intelligence: A comprehensive empirical study," *Authorea Preprints*, 2025.
- [22] E. Cancelli, T. Campari, L. Serafini, A. X. Chang, and L. Ballan, "Exploiting proximity-aware tasks for embodied social navigation," in Proceedings of the IEEE/CVF International Conference on Computer Vision, 2023, pp. 10957–10967.
- [23] H. Nishimura, B. Ivanovic, A. Gaidon, M. Pavone, and M. Schwager, "Risk-sensitive sequential action control with multi-modal human trajectory forecasting for safe crowd-robot interaction," in *IEEE/RSJ International Conference on Intelligent Robots and Systems*, 2020, pp. 11205–11212.
- [24] A. Rudenko, L. Palmieri, M. Herman, K. M. Kitani, D. M. Gavrila, and K. O. Arras, "Human motion trajectory prediction: A survey," *The International Journal of Robotics Research*, pp. 895–935, 2020.
- [25] R. Huang, H. Xue, M. Pagnucco, F. Salim, and Y. Song, "Multimodal trajectory prediction: A survey," arXiv preprint arXiv:2302.10463, 2023.
- [26] Y. Fang, Z. Wang, L. Zhang, J. Cao, H. Chen, and R. Xu, "Spiking wavelet transformer," in *European conference on computer vision*. Springer, 2024, pp. 19–37.
- [27] S. Zhang, X. Hao, Y. Tang, L. Zhang, P. Wang, Z. Wang, H. Ma, and S. Zhang, "Video-cot: A comprehensive dataset for spatiotemporal understanding of videos based on chain-of-thought," in *Proceedings of the 33rd ACM International Conference on Multimedia*, 2025, pp. 12745–12752.
- [28] Y. Tang, L. Zhang, S. Zhang, Y. Zhao, and X. Hao, "Roboafford: A dataset and benchmark for enhancing object and spatial affordance learning in robot manipulation," in *Proceedings of the 33rd ACM International Conference on Multimedia*, 2025, pp. 12706–12713.
- [29] S. K. Ramakrishnan, A. Gokaslan, E. Wijmans, O. Maksymets, A. Clegg, J. Turner, E. Undersander, W. Galuba, A. Westbury, A. X. Chang et al., "Habitat-matterport 3d dataset (hm3d): 1000 large-scale 3d environments for embodied ai," arXiv preprint arXiv:2109.08238, 2021.
- [30] Z. Gong, R. Li, T. Hu, R. Qiu, L. Kong, L. Zhang, Y. Ding, L. Zhang, and J. Liang, "Stairway to success: Zero-shot floor-aware object-goal navigation via Ilm-driven coarse-to-fine exploration," arXiv preprint arXiv:2505.23019, 2025.
- [31] L. Zhang, X. Hao, Y. Tang, H. Fu, X. Zheng, P. Wang, Z. Wang, W. Ding, and S. Zhang, "nava3: Understanding any instruction, navigating anywhere, finding anything," arXiv preprint arXiv:2508.04598, 2025.

- [32] F. Xia, W. B. Shen, C. Li, P. Kasimbeg, M. E. Tchapmi, A. Toshev, R. Martín-Martín, and S. Savarese, "Interactive gibson benchmark: A benchmark for interactive navigation in cluttered environments," *IEEE Robotics and Automation Letters*, pp. 713–720, 2020.
- [33] G. Ferrer, A. Garrell, and A. Sanfeliu, "Social-aware robot navigation in urban environments," in *Proc. of thr European Conference on Mobile Robots*, 2013.
- [34] C. Chen, Y. Liu, S. Kreiss, and A. Alahi, "Crowd-robot interaction: Crowd-aware robot navigation with attention-based deep reinforcement learning," 2019.
- [35] Y. Lu, X. Ruan, and J. Huang, "Deep reinforcement learning based on social spatial-temporal graph convolution network for crowd navigation," *Machines*, vol. 10, no. 8, p. 703, 2022.
- [36] R. Martin-Martin, M. Patel, H. Rezatofighi, A. Shenoi, J. Gwak, E. Frankel, A. Sadeghian, and S. Savarese, "JRDB: A dataset and benchmark of egocentric robot visual perception of humans in built environments," *IEEE transactions on pattern analysis and machine* intelligence, 2021.
- [37] A. D. Vuong, T. T. Nguyen, M. N. VU, B. Huang, D. Nguyen, H. T. T. Binh, T. Vo, and A. Nguyen, "Habicrowd: A high performance simulator for crowd-aware visual navigation," arXiv preprint arXiv:2306.11377, 2023.
- [38] L. Zhang, E. Xiao, Y. Zhang, H. Fu, R. Hu, Y. Ma, W. Ding, L. Chen, H. Ye, and X. Hao, "Team xiaomi ev-ad vla: Caption-guided retrieval system for cross-modal drone navigation-technical report for iros 2025 robosense challenge track 4," arXiv preprint arXiv:2510.02728, 2025.
- [39] D. Li, S. Ma, H. Hua, W. Li, J. Wang, C. W. Zhou, F. Guan, X. Li, Z. Yu, Y. Lu et al., "Vquala 2025 challenge on engagement prediction for short videos: Methods and results," in *Proceedings of* the IEEE/CVF International Conference on Computer Vision, 2025, pp. 3391–3401.
- [40] Z. Jiang, S. Zhang, J. Cao, Q. Zhang, S. Liu, Y. Fang, L. Zhang, R. Qing, and R. Xu, "Recursive cleaning for large-scale protein data via multimodal learning," bioRxiv, pp. 2024–10, 2024.
- [41] S. Y. Gadre, M. Wortsman, G. Ilharco, L. Schmidt, and S. Song, "Cows on pasture: Baselines and benchmarks for language-driven zero-shot object navigation," in *Proceedings of the IEEE/CVF Conference on Computer Vision and Pattern Recognition*, 2023, pp. 23 171–23 181.
- [42] K. Zhou, K. Zheng, C. Pryor, Y. Shen, H. Jin, L. Getoor, and X. E. Wang, "Esc: Exploration with soft commonsense constraints for zero-shot object navigation," in *International Conference on Machine Learning*, 2023, pp. 42829–42842.
- [43] L. H. Li, P. Zhang, H. Zhang, J. Yang, C. Li, Y. Zhong, L. Wang, L. Yuan, L. Zhang, J.-N. Hwang et al., "Grounded language-image pretraining," in *Proceedings of the IEEE/CVF Conference on Computer Vision and Pattern Recognition*, 2022, pp. 10965–10975.
- [44] B. Yu, H. Kasaei, and M. Cao, "L3mvn: Leveraging large language models for visual target navigation," in *IEEE/RSJ International Con*ference on *Intelligent Robots and Systems*, 2023, pp. 3554–3560.
- [45] N. H. Yokoyama, S. Ha, D. Batra, J. Wang, and B. Bucher, "Vlfm: Vision-language frontier maps for zero-shot semantic navigation," in 2nd Workshop on Language and Robot Learning: Language as Grounding, 2023.
- [46] G. Zhou, Y. Hong, and Q. Wu, "Navgpt: Explicit reasoning in visionand-language navigation with large language models," in *Proceedings* of the AAAI Conference on Artificial Intelligence, 2024, pp. 7641– 7649.
- [47] Y. Long, X. Li, W. Cai, and H. Dong, "Discuss before moving: Visual language navigation via multi-expert discussions," in *IEEE International Conference on Robotics and Automation*, 2024, pp. 17380–17387.
- [48] B. Lin, Y. Nie, Z. Wei, J. Chen, S. Ma, J. Han, H. Xu, X. Chang, and X. Liang, "Navcot: Boosting Ilm-based vision-and-language navigation via learning disentangled reasoning," *IEEE Transactions on Pattern Analysis and Machine Intelligence*, 2025.
- [49] J. Zhang, K. Wang, R. Xu, G. Zhou, Y. Hong, X. Fang, Q. Wu, Z. Zhang, and H. Wang, "Navid: Video-based vlm plans the next step for vision-and-language navigation," in *Robotics: Science and Systems*, 2024.
- [50] L. Zhang, X. Hao, Q. Xu, Q. Zhang, X. Zhang, P. Wang, J. Zhang, Z. Wang, S. Zhang, and R. Xu, "Mapnav: A novel memory representation via annotated semantic maps for vlm-based vision-andlanguage navigation," in *The 63rd Annual Meeting of the Association* for Computational Linguistics, 2025.

- [51] A.-C. Cheng, Y. Ji, Z. Yang, Z. Gongye, X. Zou, J. Kautz, E. Bıyık, H. Yin, S. Liu, and X. Wang, "Navila: Legged robot vision-languageaction model for navigation," in *Robotics: Science and Systems*, 2025.
- 52] Y. Long, W. Cai, H. Wang, G. Zhan, and H. Dong, "Instructnav: Zero-shot system for generic instruction navigation in unexplored environment," in *Conference on Robot Learning*, 2025, pp. 2049–2060.
- [53] H. Yin, X. Xu, L. Zhao, Z. Wang, J. Zhou, and J. Lu, "Unigoal: Towards universal zero-shot goal-oriented navigation," in *Proceedings* of the Computer Vision and Pattern Recognition Conference, 2025, pp. 19057–19066.
- [54] J. A. Sethian, "A fast marching level set method for monotonically advancing fronts." proceedings of the National Academy of Sciences, pp. 1591–1595, 1996.
- [55] P. E. Hart, N. J. Nilsson, and B. Raphael, "A formal basis for the heuristic determination of minimum cost paths," *IEEE transactions* on Systems Science and Cybernetics, pp. 100–107, 1968.
- [56] J. Van Den Berg, S. J. Guy, M. Lin, and D. Manocha, "Reciprocal n-body collision avoidance," in *Robotics Research: The 14th Interna*tional Symposium ISRR, 2011, pp. 3–19.
- [57] A. Chang, A. Dai, T. Funkhouser, M. Halber, M. Niessner, M. Savva, S. Song, A. Zeng, and Y. Zhang, "Matterport3d: Learning from rgb-d data in indoor environments," arXiv preprint arXiv:1709.06158, 2017.
- [58] X. Puig, E. Undersander, A. Szot, M. D. Cote, T.-Y. Yang, R. Partsey, R. Desai, A. W. Clegg, M. Hlavac, S. Y. Min et al., "Habitat 3.0: A co-habitat for humans, avatars and robots," arXiv preprint arXiv:2310.13724, 2023.